Isoscalar and isovector spin response in *sd*-shell nuclei

H. Sagawa[1,2] and T. Suzuki[3,4]
[1]*RIKEN, Nishina Center, Wako, 351-0198, Japan*
[2]*Center for Mathematics and Physics, University of Aizu, Aizu-Wakamatsu, Fukushima 965-8560, Japan*
[3]*Department of Physics, College of Humanities and Science, Nihon Univerity, Sakurajosui 3, Setagaya-ku, Tokyo 156-8550, Japan*
[4]*National Astronomical Observatory of Japan, Mitaka, Tokyo 181-8588, Japan*

(Received 26 July 2017; revised manuscript received 25 March 2018; published 31 May 2018)

The spin magnetic-dipole transitions and the neutron-proton spin-spin correlations in *sd*-shell even-even nuclei with $N = Z$ are investigated by using shell-model wave functions taking into account enhanced isoscalar (IS) spin-triplet pairing as well as the effective spin operators. It was shown that the IS pairing and the effective spin operators gives a large quenching effect on the isovector (IV) spin transitions to be consistent with data observed by (p, p') experiments. On the other hand, the observed IS spin strengths show much smaller quenching effect than expected by the calculated results. The IS pairing gives a substantial quenching effect on the spin magnetic-dipole transitions, especially on the IV transitions. Consequently, an enhanced IS spin-triplet pairing interaction enlarges the proton-neutron spin-spin correlation deduced from the difference between the IS and the IV sum-rule strengths. The β-decay rates and the IS magnetic moments of the *sd* shell are also studied in terms of the IS pairing as well as the effective spin operators.

DOI: 10.1103/PhysRevC.97.054333

I. INTRODUCTION

The spin-isospin response and spin-isospin-dependent interactions in nuclei are fundamental important problems in nuclear physics and astrophysics. The Gamow–Teller (GT) transition is an "allowed" charge-exchange transition induced by the operator $\vec{\sigma} t_{\pm}$, while the magnetic-dipole ($M1$) transition, defined in a no-charge-exchange channel, involves both the spin and the orbital angular-momentum operators [1]. It has been argued that these spin-isospin responses need to be quenched in order to reproduce the experimental values [2,3]. The experimental GT and $M1$ strengths or the spin part of the magnetic moments are quenched compared with the relevant theoretical predictions by shell-model and random-phase approximations [4–9]. It was also pointed out that descriptions of GT and $M1$ transition strengths as well as magnetic moments in nuclei have been much improved with the inclusion of the tensor components in the shell-model interactions [10–14].

The quenching effect of spin-isospin responses influences many physical and astrophysical processes such as the neutrinoless double-β decays ($0\nu\beta\beta$) [15], the spin susceptibility of asymmetric nuclear matter [16], neutrino-nucleus reaction cross sections [17], the dynamics and nucleosynthesis in core-collapse supernovae explosions [18], the cooling of O-Ne-Mg cores in stars with mass $8M_{\odot}$–$10M_{\odot}$ [19–21] as well as that of prototype neutron stars [22], and the spin-response to strong magnetic fields in magnetars [23].

The quenching phenomena of magnetic moments and GT strengths have been extensively studied by taking into account the mixings of particle-hole (p-h) configurations, meson exchange currents, and the coupling to the Δ resonances [2,3,24–26]. Various contributions have been found to be important for the quenching. On the quenching of the GT sum rule, $3(N - Z)$ [4], there has been a serious question whether the effect independent to nuclear structure such as the coupling to Δ is a dominant contribution [25,26]. After a long debate [27], experimental investigations by charge-exchange (p,n) and (n,p) reactions on ^{90}Zr have revealed that about 90% of the GT sum-rule strength exists in the energy region up to $E_x = 50$ MeV [6,28]. This demonstrates the importance of the two-particle two-hole ($2p$-$2h$) configuration mixings due to the central and tensor forces [24], although the coupling to Δ is not completely excluded.

Recently, isoscalar (IS) and isovector (IV) spin $M1$ transitions have been investigated by high-resolution proton inelastic-scattering measurements at $E_p = 295$ MeV [29]. The IV spin $M1$ transitions induced by the operator $\vec{\sigma} t_z$ can be regarded as analogous to GT transitions, while the IS spin $M1$ transitions are free from the coupling to Δ and the quenching of IS strength should be due to the couplings to higher p-h configurations. The quenchings of IS and IV spin operators have been pointed out to be similar by various theoretical studies [30]. However, the proton inelastic-scattering experiments have shown that the IS quenching is substantially smaller than the IV quenching for several $N = Z$ *sd*-shell nuclei [29].

We recently studied this problem by taking into account the IS spin-triplet pairing interaction in $N = Z$ *sd*-shell nuclei to see if the difference of the quenching between IS and IV transitions can be obtained [31]. The IS pairing is found to induce more quenching in IV spin $M1$ transitions than IS transitions. The IS spin-triplet pairing correlations have been reported to play an important role in enhancing the GT strength near the ground states of daughter nuclei with mass $N \sim Z$ [32–35]. At the same time, the total sum rule of the GT strength is quenched by ground-state correlations due to the IS pairing [36]. The IS paring is also found to be important to reduce $0\nu\beta\beta$ decay matrix elements [37].

In this paper, we extend our study in Ref. [31] and investigate the IS and IV spin $M1$ responses in more detail based on shell-model effective interactions with enhanced IS pairing correlations for the same set of $N = Z$ sd-shell nuclei as those observed in Ref. [29]. The structure of the effective $M1$ and GT operators are also explored. Simultaneous calculations of these responses within the same nuclear model may be advantageous to distinguish the effect of the higher-order configurations from the Δ-hole coupling. We discuss also the effect of IS spin-triplet pairing interaction on the spin responses and the proton-neutron spin-spin correlations in the ground states of $N = Z$ nuclei.

The spin $M1$ operators are introduced in Sec. II and their sum rules are also defined. Section III is devoted to the shell-model calculations of $N = Z$ even-even nuclei in comparisons with available experimental data by (p, p') reactions. The accumulated sum-rule values of IS and IV spin transitions are extracted in Sec. IV. The proton-neutron spin-spin correlations are also discussed in terms of the IS spin-triplet pairing correlations. The β-decay rates and IS magnetic moments in the sd shell are studied in the same context of the shell-model calculations in Sec. V. The summary is given in Sec. VI.

II. SPIN $M1$ OPERATORS AND SUM RULES

The bare IS and IV spin $M1$ operators are given by

$$\hat{O}_{\rm IS} = \sum_k \vec{\sigma}(k), \tag{1}$$

$$\hat{O}_{\rm IV} = \sum_k \vec{\sigma}(k)\tau_z(k), \tag{2}$$

while the GT charge-exchange excitation operators are expressed as

$$\hat{O}_{\rm GT} = \sum_k \vec{\sigma}(k)t_\pm(k). \tag{3}$$

The sum-rule values for the $M1$ spin transitions are defined by

$$S(\vec{\sigma}) = \sum_f \frac{1}{2J_i+1}|\langle J_f||\hat{O}_{\rm IS}||J_i\rangle|^2, \tag{4}$$

$$S(\vec{\sigma}\tau_z) = \sum_f \frac{1}{2J_i+1}|\langle J_f||\hat{O}_{\rm IV}||J_i\rangle|^2. \tag{5}$$

For the GT transition, the sum-rule value is defined in a similar way to the $M1$ transitions as

$$S(\vec{\sigma}t_\pm) = \sum_f \frac{1}{2J_i+1}|\langle J_f||\hat{O}_{\rm GT}||J_i\rangle|^2, \tag{6}$$

which gives the well-known model independent sum rule,

$$S(\vec{\sigma}t_-) - S(\vec{\sigma}t_+) = 3(N-Z). \tag{7}$$

According to Ref. [29], the proton-neutron spin-spin correlation is obtained from the sum-rule values (4) and (5) as

$$\Delta_{\rm spin} = \tfrac{1}{16}[S(\vec{\sigma}) - S(\vec{\sigma}\tau_z)] = \langle J_i|\vec{S}_p\cdot\vec{S}_n|J_i\rangle, \tag{8}$$

where $\vec{S}_p = \sum_{k\in p}\vec{s}(k)$ and $\vec{S}_n = \sum_{k\in n}\vec{s}(k)$. The correlation value is 0.25 and -0.75 for a pure spin-triplet and a spin-singlet proton-neutron pair, respectively. The former corresponds to the ferromagnet limit of the spin alignment, while the latter is the antiferromagnetic one.

III. SHELL-MODEL CALCULATIONS WITH EFFECTIVE OPERATORS AND ISOSCALAR PAIRING CORRELATIONS

The shell-model calculations are performed in full sd-shell-model space with the USDB interaction [38]. Among the effective interactions of the USD family, USD [39], USDA [38], and USDB [38], the results of spin excitations with $J^\pi = 1^+$ are quite similar to each other both in excitation energies and transition strengths for collective states with large transition strengths. Hereafter, we present results based on the USDB interaction. To take into account the effects of higher-order configuration mixings as well as meson exchange currents and the Δ-isobar effect, effective operators are commonly adopted in the study of magnetic moments, GT transitions, and spin- and spin-isospin-dependent β decays.

IV magnetic transitions in sd-shell nuclei and GT transitions have been studied extensively in experiments and theories. On the other hand, experimental evidence of IS magnetic transitions is not well known so far except for recent experimental data by Matsubara *et al.* [29]. In the literature [2,3,40], the effective operators have been introduced to mimic the effects of higher-order configuration mixings, meson-exchange currents, Δ-isobar coupling and the relativistic corrections. For the spin operators, the effective operators read for the IS operator

$$\hat{O}^{\rm eff}_{\rm IS} = f_s^{\rm IS}\vec{\sigma} + f_l^{\rm IS}\vec{l} + f_p^{\rm IS}\sqrt{8\pi}[Y_2\times\vec{\sigma}]^{(\lambda=1)}, \tag{9}$$

and also for the IV spin operator,

$$\hat{O}^{\rm eff}_{\rm IV} = f_s^{\rm IV}\vec{\sigma}\tau_z + f_l^{\rm IV}\vec{l}\tau_z + f_p^{\rm IV}\sqrt{8\pi}[Y_2\times\vec{\sigma}]^{(\lambda=1)}\tau_z, \tag{10}$$

where $f_\alpha^{\rm IS}$ ($f_\alpha^{\rm IV}$), $\alpha = s, l, p$ are the effective coefficients of IS (IV) spin, orbital an spin-tensor operators. The summation of index k in Eqs. (1)–(3) is discarded in the effective operators. The effective coefficients for the IS spin operator obtained by Towner are $f_s^{\rm IS} = 0.745$, $f_l^{\rm IS} = 0.0526$, and $f_p^{\rm IS} = -0.0157$. For the IV part, Towner obtained the corrections for the spin, orbital, and the spin-tensor operators of GT transitions of $1d$ orbit as

$$\hat{O}^{\rm eff}_{\rm GT} = (1+\delta g_s)\vec{\sigma}t_\pm + \delta g_l\vec{l}t_\pm + \delta g_p\sqrt{8\pi}[Y_2\times\vec{\sigma}]^{(\lambda=1)}t_\pm, \tag{11}$$

with

$$\delta g_s = -0.139, \quad \delta g_l = 0.0103, \quad \delta g_p = 0.0283, \tag{12}$$

due to the various higher-order effects. In the shell-model calculations with USD interaction, the IV spin and charge-exchange GT excitations are the same features since no isospin-breaking interaction such as Coulomb interaction and charge-symmetry-breaking forces is included. We adopt the GT effective operators for IV spin transitions. For the IS part, the quenching factor for the spin operator is introduced to check the sensitivity of transition strength on the effective operator. The effective operators for IS orbital and spin tensor are not introduced in the present study.

In the following calculations, we introduce effective interactions with enhanced IS spin-triplet pairing matrices on top of the USDB interaction. The interactions USDB* and USDB** denote the effective interactions whose IS pairing matrices are enhanced by multiplying a factor 1.1 and 1.2, respectively. Results with effective operators are marked by "qis" or "qiv" for the IS and IV transitions, respectively. For the IS case, we perform four different versions of calculations:

(1) USDB: the original interaction with the bare spin operator.
(2) USDB*: the IS spin-triplet pairing matrices are enhanced multiplying by a factor 1.1 on the relevant matrix elements of USDB interaction. The bare spin operator is adopted.
(3) USDB*qis: the IS spin-triplet pairing matrices are enhanced multiplying by a factor 1.1. The IS spin operator is 10% quenched: $f_s^{\rm IS} = 0.9$.
(4) USDB**qis: the IS spin-triplet pairing matrices are enhanced multiplying by a factor 1.2. The IS spin operator is 10% quenched: $f_s^{\rm IS} = 0.9$.

For the IV case, we perform three different calculations:

(1) USDB: the original interaction with the bare spin operator.
(2) USDB*qiv: the IS spin-triplet pairing matrices are enhanced multiplying by a factor 1.1. The effective IV spin operator (11) is adopted.
(3) USDB**qiv: the IS spin-triplet pairing matrices are enhanced multiplying by a factor 1.2. The effective IV spin operator (11) is adopted.

In Ref. [30], the effective operators for $M1$ and GT transitions are introduced on top of the USDB interaction. These effective operators have essentially the same features as those of Towner's. In this paper, we adopt the Towner's effective operators to examine their roles on the spin $M1$ transitions.

A. ^{20}Ne

Figures 1(a) and 2(a) show the energy spectra of the IS spin excitations and their cumulative sums, respectively, in ^{20}Ne. The IS spin-triplet matrix elements are enhanced by a factor 1.1 for USDB* and USDB*qis, and by a factor 1.2 for the USDB**qis case. Together with the enhancement of IS pairing, the quenched spin operator is introduced in the cases USDB*qis and USDB**qis with $f_s^{\rm IS} = 0.9$. The calculated results are smoothed by a Lorentzian weighting factor with the width of 0.5 MeV to guide the eye. The shell-model results with USDB give 1^+ states at $E_x = 12.64$ and 14.98 MeV with $B(\sigma) = 0.360$ and 0.519, respectively. The USDB**qis results with the enhanced pairing and the quenched spin operator are also shown in the same figure. The lowest state in the case of USDB**qis is found at $E_x = 12.55$ MeV with a smaller strength $B(\sigma) = 0.178$, which is a half of USDB one. The higher-energy strength is fragmented into three peaks at $E_x \sim$ 14.5 and 16.6 MeV with the summed strength $B(\sigma) = 0.19$. The accumulated values are shown in Fig. 2 for four cases USDB, USDB*, USDB*qis, and USDB*qis. In ^{20}Ne, the accumulated sum increases up to $E_x \sim 20$ MeV. The enhanced IS pairing in USDB* gives about 10% quenching compared with USDB results, while more-enhanced IS pairing in USDB**qis gives further quenching compared with USDB*qis. In the (p, p') data, the IS strengths are not found so far.

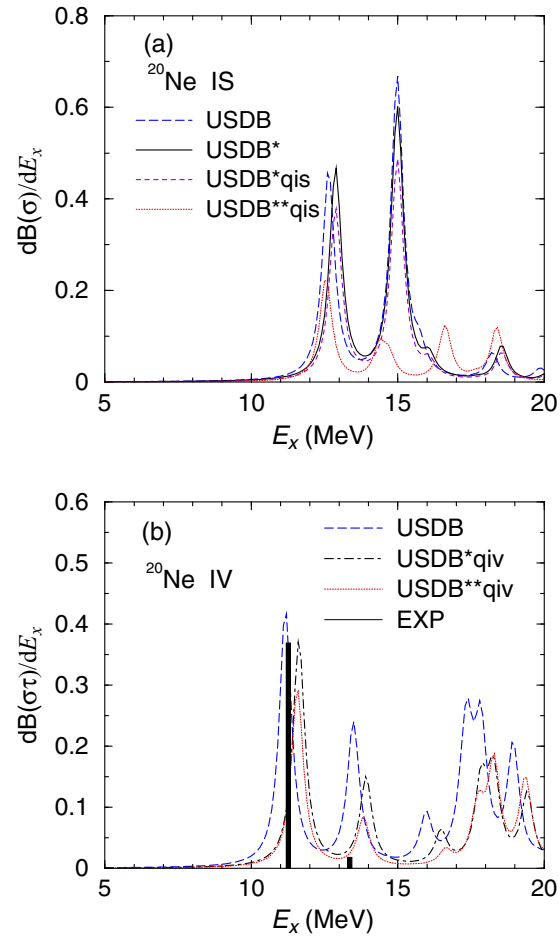

FIG. 1. IS (top) and IV spin-$M1$ (bottom) transition strengths in ^{20}Ne. Shell-model calculations are performed in the full sd-shell-model space with a USDB effective interaction. For the IS case, the USDB* and USDB*qis have the 10% enhanced IS spin-triplet interaction, while USDB**qis has 20% enhanced ones. The quenching factor for the IS spin operator $f_s^{\rm IS} = 0.9$ is introduced for USDB*qis and USDB**qis calculations. For the results of the IV spin-$M1$ transitions, an effective IV spin operator (11) is adopted in USDB*qiv and USDB**qiv cases. The IS spin-triplet interaction is enhanced by multiplying the relevant matrix elements by factors 1.1 and 1.2 in the cases of USDB*qiv and USDB**qiv, respectively, together with the effective operator. Calculated results are smoothed by taking a Lorentzian weighting factor with the width of 0.5 MeV, while the experimental data are shown in the units of $B(\sigma)$ for the IS excitations and $B(\sigma\tau)$ for the IV excitations. Experimental data are taken from Ref. [29].

The results of IV spin response are shown in Figs. 1(b) and 2(b). The original USDB gives IV strength at $E_x = 11.16$ and 13.49 MeV with $B(\sigma\tau) = 0.331$ and 0.183, respectively, below $E_x = 15$ MeV. The excitation energies of these two peaks are shifted to higher energies 11.62 and 13.92 MeV in the case of enhanced IS pairing USDB*qiv. Comparing with

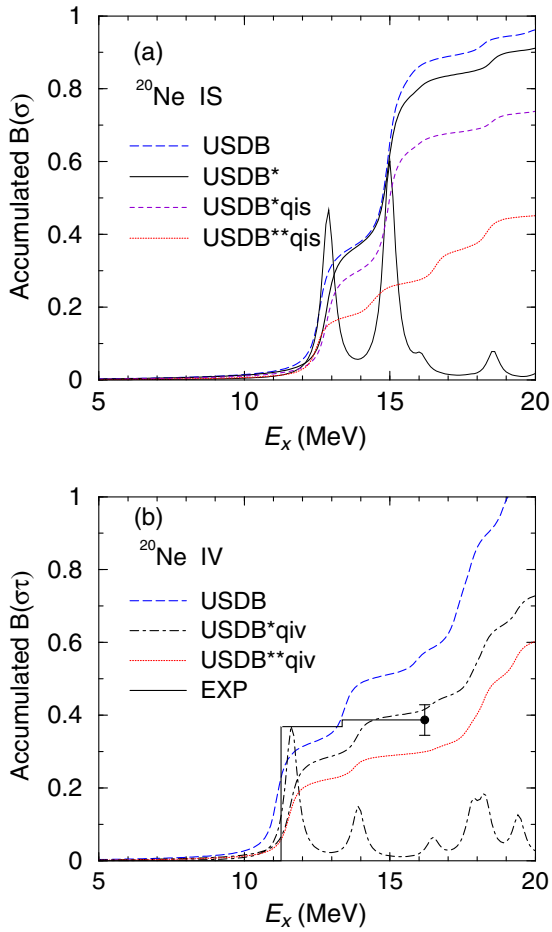

FIG. 2. Cumulative sums of the IS spin-$M1$ strength (top) and the IV spin-$M1$ strength (bottom) as a function of the excitation energy in ^{20}Ne. The calculated energy spectra are also shown for USDB* in the IS channel and for USDB*qiv in the IV channel. Calculated results are smoothed in the same manner as in Fig. 1. Dot with a vertical error bar denotes the experimental accumulated sum of the strengths. See the text and the caption to Fig. 1 for details.

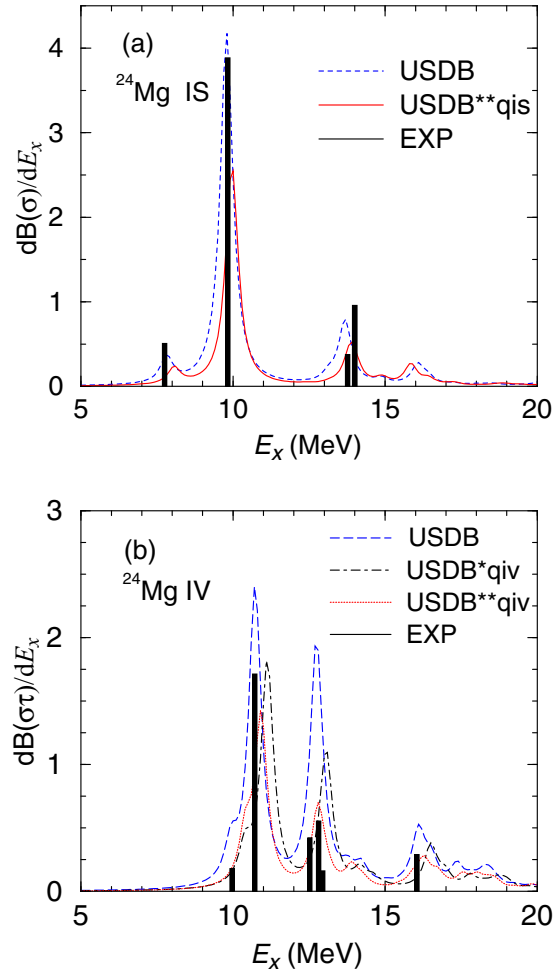

FIG. 3. IS (top) and IV spin-$M1$ (bottom) transition strengths in ^{24}Mg. See text and caption to Fig. 1 for details.

the results of USDB*qiv, the USDB**qiv gives essentially the same excitation energies for 1^+ spectra, while the $B(\sigma\tau)$ are decreased from 0.292 to 0.230 for the first peak and from 0.113 to 0.0627 for the second peak. The calculated results give large strength also in the energy region above $E_x = 15$ MeV. The accumulated sums are shown in Fig. 2(b). Up to $E_x =$ 16 MeV, the accumulated sums are 0.577, 0.406, and 0.293 for USDB, USDB*qiv, and USDB**qiv, respectively. Due to the strong IS pairing and the effective IV spin operator, the accumulated strength decrease by 30% for USDB*qiv and 50% for USDB**qiv. The (p, p') experiments found two IV states at $E_x = 11.26$ and 13.36 MeV with $B(\sigma\tau) = 0.369$ and 0.018, respectively. The summed strength 0.387 is comparable with the result of USDB*qiv.

B. ^{24}Mg

Figures 3 and 4 show the energy spectra of the spin excitations and their cumulative sums, respectively, in ^{24}Mg. For the IS case, the experimental data give the strong spin $M1$ strength at $E_x = 9.828$ MeV with $B(\sigma) = 3.886 \pm 1.102$. The shell-model results with USDB give IS 1^+ state at $E_x =$ 9.818 MeV with $B(\sigma) = 3.278$. In the (p, p') data, other IS strengths are also found at 7.748 MeV with $B(\sigma) = 0.508$ and at $E_x \sim 14$ MeV with $B(\sigma) \sim 1.2$. The calculated results reproduce strong $M1$ states at very similar energies $E_x =$ 7.82 and 13.7 MeV with $B(\sigma) = 0.24$ and 0.59, respectively. The calculations with USDB show also the same amount of $B(\sigma)$ value as the experimental data around $E_x =$14 MeV. The summed strength up to $E_x = 16$ MeV is $B_{\rm expt}(\sigma : E_x \leqslant 16\ {\rm MeV}) = 5.061 \pm 1.166$, while the calculated sum is $B_{\rm calc}(\sigma : E_x \leqslant 16\ {\rm MeV}) = 4.256$. The calculated results of USDB**qis changes only slightly the excitation energies of 1^+ states by about 100–200 keV, while the summed $B(\sigma)$ value is decreased by 30%.

The experimental analysis show a strong IV spin strength at $E_x = 10.71$ MeV with $B(\sigma\tau) = 1.714$. The calculation gives at $E_x = 10.723$ MeV with $B(\sigma\tau) = 1.854$. Experimental data show also substantial strength around $E_x =$ 12.8 MeV with $B(\sigma) \sim 1$ and at $E_x = 9.968$ and 16.046 MeV with $B(\sigma\tau) = 0.18$ and 0.29, respectively. The calculated results give large strengths at $E_x = 9.939$ MeV and

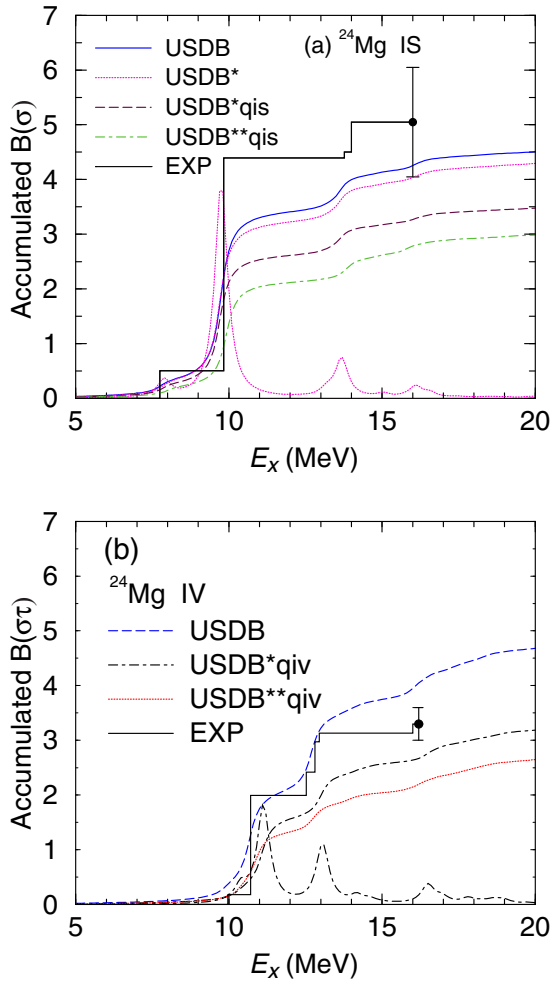

FIG. 4. Cumulative sum of the IS spin-$M1$ strength (top) and the IV spin-$M1$ strength (bottom) as a function of excitation energy in ^{24}Mg. See text and caption to Fig. 2 for details.

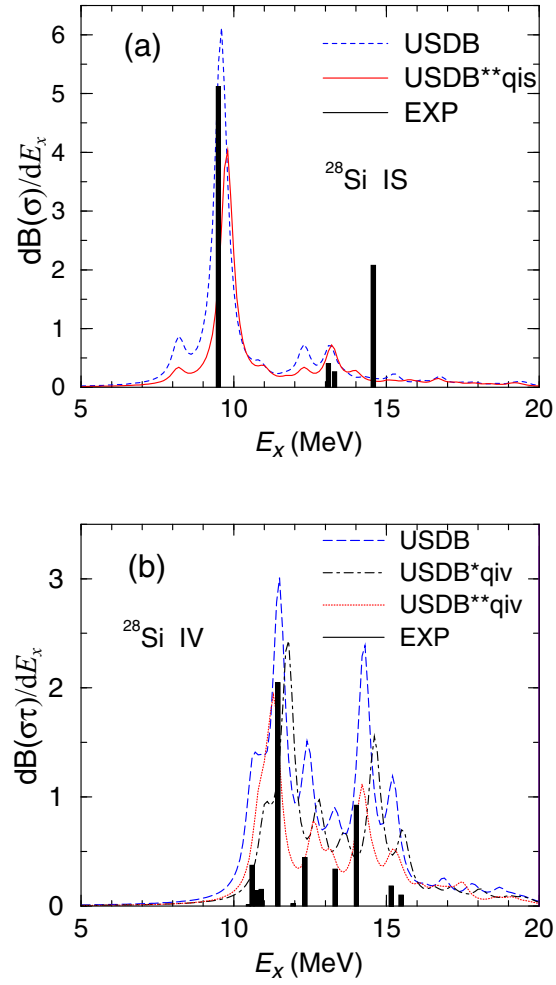

FIG. 5. IS (top) and IV spin-$M1$ (bottom) transition strengths in ^{28}Si. See caption to Fig. 1 and text for details.

10.75 MeV with $B(\sigma\tau) = 0.238$ and 1.521, respectively. The experimental summed strength is $B_{\rm expt}(\sigma\tau : E_x \leqslant 16\ {\rm MeV}) = 3.180 \pm 0.236$, while the calculated value is $B_{\rm calc}(\sigma\tau : E_x \leqslant 16\ {\rm MeV}) = 3.855$. There are about 20% quenching in the empirical sum-rule strength of IV spin excitations below $E_x = 16$ MeV compared with USDB results with the bare spin operator. The USDB*qiv and USDB**qiv results with the effective spin operator show about 30 and 40% quenching of the accumulated strength up to $E_x = 16$ MeV, respectively.

We study the effects of the isospin-mixing in ^{24}Mg. The 1^+, $T = 0$ states at $E_x = 7.747$ MeV and 9.827 MeV are mixed with the 1^+, $T = 1$ state at $E_x = 9.966$ MeV by the two-body Coulomb interaction $V_{\rm CD}$ [41]. Using the mixing amplitudes obtained by [41]

$$\frac{\langle T = 1|V_{\rm CD}|T = 0\rangle}{\Delta E} \quad \text{with } \langle {\rm T} = 1|{\rm V_{CD}}|{\rm T} = 0\rangle = 49\ {\rm keV},$$

an enhancement is obtained for $S(\vec{\sigma})$ from 4.256 to 4.492, and a reduction is shown for $S(\vec{\sigma}\tau_z)$ from 3.856 to 3.652. These changes give an enhancement of $\Delta_{\rm spin}$ by 0.026 for USDB. These effects are favorable and consistent with the experimental data although their magnitudes are not so large.

C. ^{28}Si

The calculated results of IS spin states are shown in Figs. 5(a) and 6(a). The calculated results give an IS 1^+ state at $E_x = 9.6$ MeV with USDB interaction, which reproduces well the experimental IS 1^+ state with a strong spin transition at $E_x = 9.58$ MeV exhausting about 70% of the total IS strength. Another strong state is observed at $E_x = 14.571$ MeV with $B(\sigma) = 2.075 \pm 0.621$, while the calculation shows no sign of a strong $B(\sigma)$ transition above $E_x = 14$ MeV. Other IS spin transitions are found experimentally at $E_x \sim 13$ MeV with $B(\sigma) \sim 0.7$. The calculations show also the IS spin strength of $B(\sigma) \sim 1.0$ at $E_x = (12.3$–$13.2)$ MeV. The accumulated empirical IS strength below $E_x = 16$ MeV is $B_{\rm expt}(\sigma : E_x \leqslant 16\ {\rm MeV}) = 6.489 \pm 1.604$, while the calculated results are $B_{\rm calc}(\sigma : E_x \leqslant 16\ {\rm MeV}) = 6.816$, 6.611, 5.355 and 4.562 for USDB, USDB*, USDB*qis, and USDB**qis, respectively. The $B_{\rm calc}(\sigma : E_x \leqslant 16\ {\rm MeV})$ values show 3%, 21%, and 33% quenching for the USDB*, USDB*qis, and USDB**qis interactions, respectively, compared with USDB results.

The IV spin response is shown in Figs. 5(b) and 6(b). The gross structure of the empirical IV spin response is well reproduced by the calculations based on the USDB interaction.

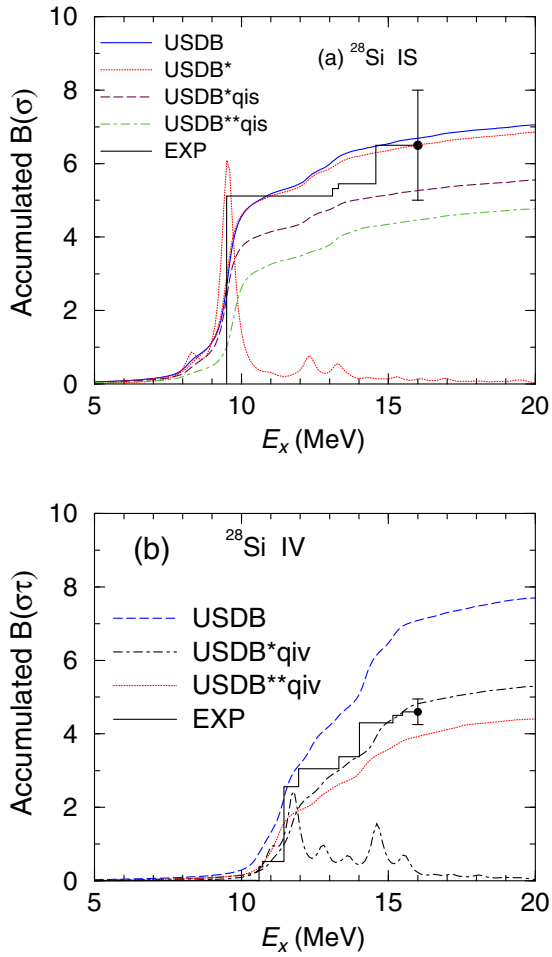

FIG. 6. Cumulative sum of the IS spin-$M1$ strength (top) and the IV spin-$M1$ strength (bottom) as a function of the excitation energy in ^{28}Si. See caption to Fig. 2 and text for details.

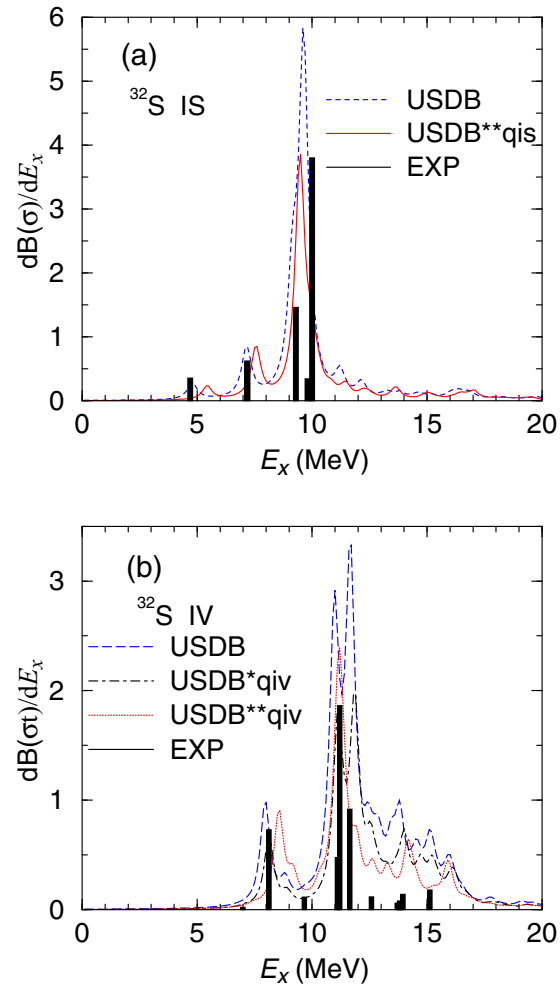

FIG. 7. IS (top) and IV spin-$M1$ (bottom) transition strengths in ^{32}S. See caption to Fig. 1 for details.

The empirical IV spin strength is rather fragmented, while two IV 1^+ states with strong spin strengths of $B(\sigma\tau) = 2.05$ and 0.92 are reported at $E_x = 11.45$ and 14.01 MeV, respectively. Calculated results show also largely fragmented IV spin strength and two strong strengths are found at $E_x = 11.48$ and 14.26 MeV with $B(\sigma\tau) = 2.165$ and 1.773, respectively, with the USDB interaction. The empirical accumulated IV strength is $B_{\rm expt}(\sigma\tau : E_x \leqslant 16\ {\rm MeV}) = 4.59 \pm 0.222$, while the calculated one is $B_{\rm calc}(\sigma\tau : E_x \leqslant 16\ {\rm MeV}) = 7.34$, 5.03, and 4.03 for the USDB, USDB*qiv, and USDB**qiv cases, respectively. In the spin IV sum-rule value, we see a large quenched spin factor $q_s^{IV}({\rm eff}) \equiv \sqrt{B_{\rm expt}(\sigma\tau)/B_{\rm calc}(\sigma\tau : {\rm USDB})} = 0.79$, which is close to the ratio of accumulated values of USDB*qiv to USDB. It is pointed out also in Ref. [31] that the enhanced IS pairing multiplying a factor 1.2 on the IS pairing matrices reduces the IV spin transition strength, corresponding to the renormalization factor of $f_s^{\rm IV} = 0.87$ for the accumulated IV spin strength. On the other hand, the same enhanced IS pairing gives the IS quenching factor $f_s^{\rm IS} = 0.91$. This difference between IS and IV spin response induces a positive value for the proton-neutron spin-spin correlations in the ground state. This point will be discussed more in Sec. IV.

D. ^{32}S

For the IS case shown in Fig. 7(a), the experimental data show a strong state at $E_x = 9.956$ MeV with $B(\sigma) = 3.810 \pm 1.118$. The corresponding state is found in the calculated results at $E_x = 9.632$ MeV with $B(\sigma) = 4.312$. Another strong IS transition was found at $E_x = 9.297$ MeV with $B(\sigma) = 1.461 \pm 0.436$, while the calculations show a state at $E_x = 9.154$ MeV with $B(\sigma) = 1.293$ MeV. There are two IS states observed below $E_x = 7.2$ MeV. The calculations found also two states at the same energy region with almost the same $B(\sigma)$ values as the observed ones. The observed IS sum rule strength is $B_{\rm expt}(\sigma : E_x \leqslant 16\ {\rm MeV}) = 6.414 \pm 1.227$, while theoretically $B_{\rm calc}(\sigma : E_x \leqslant 16\ {\rm MeV}) = 7.623$ in Fig. 8(a). We can see a small quenching effect corresponding to $f_s^{\rm IS}({\rm eff}) = 0.92$ for the sum-rule strength below $E_x = 16$ MeV.

The IV response in ^{32}S is shown Fig. 7(b). The IV spin strength is concentrated at $E_x \sim 11.3$ MeV having 80% of the total strength below $E_x = 16$ MeV. The calculated results show also very large fraction of the total strength of about 87% of the total strength. Another strong state is found experimentally at $E_x = 8.125$ MeV with $B(\sigma\tau) = 0.730 \pm 0.040$, while the calculations show a state at $E_x = 7.959$ MeV

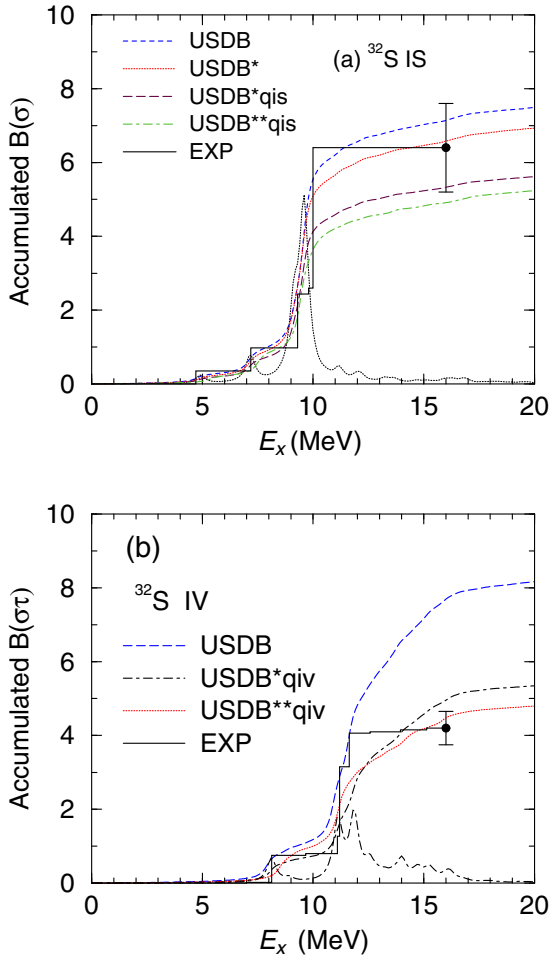

FIG. 8. Cumulative sum of the IS spin-$M1$ strength (top) and the IV spin-$M1$ strength (bottom) as a function of excitation energy in ^{28}Si. See caption to Fig. 2 for details.

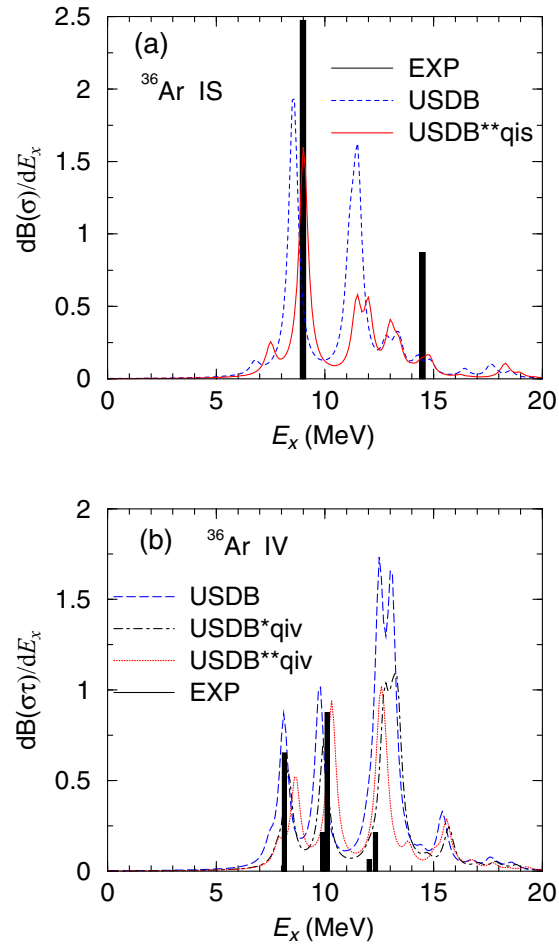

FIG. 9. IS (top) and IV spin-$M1$ (bottom) transition strengths in ^{36}Ar. See caption to Fig. 1 for details.

with $B(\sigma\tau) = 0.743$. The agreement between theory and experiment is quite satisfactory as far as the gross feature of IV spin response is concerned. The accumulated strength of IV transitions is $B_{\rm expt}(\sigma\tau : E_x \leqslant 16\ {\rm MeV}) = 4.120 \pm 0.407$, while the calculated results are $B_{\rm calc}(\sigma\tau : E_x \leqslant 16\ {\rm MeV}) = 7.993$ in Fig. 8(b). We see a large quenching for IV case with $q_s^{IV}({\rm eff}) = 0.72$. The results USDB**qiv with the enhanced IS pairing and the effective IV spin operator give good account of the accumulated strength.

E. ^{36}Ar

The IS spin response in ^{36}Ar is given in Fig. 9(a). The experiments found two states: $E_x = 8.985$ and 14.482 MeV with $B(\sigma) = 2.473 \pm 1.045$ and 0.872 ± 0.342, respectively. The shell-model results of USDB show a strong IS strength at $E_x = 8.551$ MeV with $B(\sigma) = 1.558$. Above $E_x = 10$ MeV, the calculated IS strength is rather fragmented with the summed $B(\sigma) \sim 2$ in the energy region $E_x = (11$–$15)$ MeV. The experimental accumulated strength in Fig. 10(a) is $B_{\rm expt}(\sigma : E_x \leqslant 16\ {\rm MeV}) = 2.910 \pm 1.091$, while the calculated value is $B_{\rm calc}(\sigma : E_x \leqslant 16\ {\rm MeV}) = 3.753$. We see a small quenching with the factor $q_s^{IS}({\rm eff}) = 0.88$.

The IV spin strength is shown in Fig. 9(b). Experimental data show two large IV strengths at $E_x = 8$ and 10 MeV having 33% and 55% of the observed total strength below $E_x = 16$ MeV. The calculated USDB results show also two strong spin strengths at $E_x = 8.11$ MeV and $E_x = 9.8$ MeV with $B(\sigma\tau) = 0.648$ and 0.788, respectively. The calculations show another strong IV transition strength with $B(\sigma\tau) \sim 2.3$ at $E_x \sim 13$ MeV, while experimental data observed a small strength with $B(\sigma\tau) \sim 0.3$ around $E_x = 12$ MeV. The observed accumulated strength in Fig. 10(b) is $B_{\rm expt}(\sigma\tau : E_x \leqslant 16\ {\rm MeV}) = 1.986 \pm 0.143$, while the calculated one is $B_{\rm calc}(\sigma\tau : E_x \leqslant 16\ {\rm MeV}) = 4.125$. The quenching is rather large with the factor $q_s^{IV}({\rm eff}) = 0.69$ for the IV case so that the results of USDB**qiv in Fig. 10(b) give the closest value to the empirical one.

F. ^{12}C

For a reference, we mention the IS and IV 1^+ states in ^{12}C, although it is a p-shell nucleus and not a sd-shell nucleus. In ^{12}C, IS and IV 1^+ states are observed at $E_x = 12.71$ and 15.11 MeV, respectively. The $B(M1)$ values are extracted from (e,e') scattering experiments to be $B(M1) = 0.0402$ and 2.679 in terms of nuclear magneton $(e\hbar/2mc)^2$ [42]. The shell-model

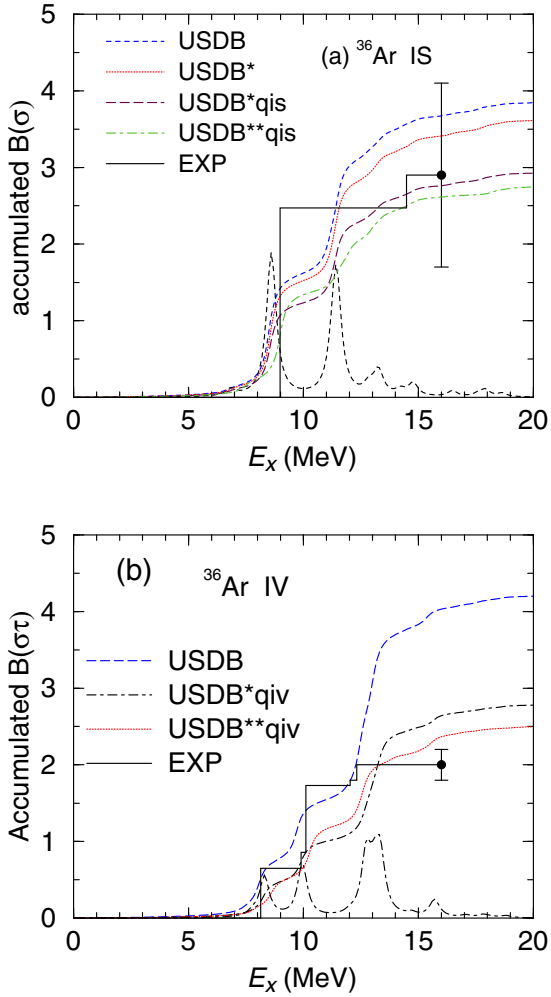

FIG. 10. Cumulative sum of the IS spin-$M1$ strength (top) and the IV spin-$M1$ strength (bottom) as a function of excitation energy in ^{28}Si. See caption to Fig. 2 for details.

calculations with CKPOT interaction give $B(M1) = 0.01434$ and 2.314 in units of nuclear magneton at $E_x = 12.45$ and 15.09 MeV, respectively, with the bare magnetic transition operators. A recent p-sd shell Hamiltonian, SFO [10], gives $B(M1) = 0.0131\mu_N^2$ and $2.515\mu_N^2$ for the IS and IV transitions, respectively. The model space of SFO is the p-sd shell and the excitations from the p shell to the sd shell are included up to $2\hbar\omega$. It is noticed that the experimental value is about three times larger than the calculated value for the IS 1^+ state at $E_x = 12.71$ MeV, while the calculated value for the IV state is close to the experimental value. The (p, p') data were reported for the two 1^+ states to be $B(\sigma) = 3.174 \pm 0.842$ at $E_x = 12.71$ MeV and $B(\sigma\tau) = 1.909 \pm 0.094$ at $E_x = 15.11$ MeV, respectively. The shell-model results with SFO are $B(\sigma) = 1.516$ and $B(\sigma\tau) = 1.937$, respectively. The proton inelastic-scattering data of the state at $E_x = 12.71$ MeV show also a factor two larger value than the shell-model results. The isospin mixing between the two 1^+ state has been discussed as an origin of the enhancement of IS spin matrix element. A large isospin mixing was claimed to enhance IS magnetic transition observed by electron scattering.

The same effect is expected for $B(\sigma)$. When the IS 1^+ at 12.71 MeV and IV 1^+ at 15.11 MeV states are mixed by the isospin-mixing effect,

$$|1^+, 12.71\ \text{MeV}\rangle = \sqrt{1-a^2}|1^+, T=0\rangle + a|1^+, T=1\rangle,$$
$$|1^+, 15.11\ \text{MeV}\rangle = \sqrt{1-a^2}|1^+, T=1\rangle - a|1^+, T=0\rangle, \quad (13)$$

we get an enhancement of $B(\sigma)$ as well as a reduction of $B(\sigma\tau)$. $B(\sigma)$ is enhanced from 1.516 to 1.714 while $B(\sigma\tau)$ is reduced from 1.937 to 1.750 and the mixing amplitude $a = 0.056$ [43]. The proton-neutron spin-spin correlation Δ_{spin} in Eq. (8) is found to be enhanced by 0.024. Although the isospin-mixing gives rise to favorable effects, it is still not enough to reproduce the experimental value of $B(\sigma)$.

IV. ACCUMULATED STRENGTH OF ISOSCALAR AND ISOVECTOR SPIN $M1$ EXCITATIONS

Figure 11 shows the sum-rule values of $S(\vec{\sigma})$ and $S(\vec{\sigma}\tau_z)$ for the variations of interactions, respectively. The 10% enhanced IS pairing in USDB* give a small quenching effect on the accumulated IS sum-rule value; about 5% on average and at most 7% in ^{32}S and ^{36}Ar. With the quenching factor $f_s^{\text{IS}} = 0.9$ in USDB*qis, the IS accumulated strength is further decreased by 22%–25% compared with the original value by USDB interaction. The decrease of the accumulated IS value is going down further to be 29%–33% in the case of USDB**qis with the 20% enhanced IS pairing. Compared with USDB calculations, the empirical accumulated IS values are 20% enhanced in ^{24}Mg and gradually quenched from $A = 28$ to 36; 0.95, 0.88, and 0.77 in ^{28}Si, ^{32}S, and ^{36}Ar, respectively. Thus the quenching effect in the experimental data is rather small and at most 23% of the USDB calculations with the bare spin operator.

The IV accumulated sum-rule values up to $E_x = 16$ MeV are shown in Fig. 11. The IS pairing interactions are enhanced by factors of 1.1 for USDB*qiv and 1.2 for USDB**qiv, respectively, with the effective operators from Ref. [3]. The results of USDB*qiv give 31%–36% quenched sum-rule values, while the stronger IS pairing in USDB**qiv gives additional quenching of the strength, i.e., 41%–45% quenching of the summed strength. The empirical values show also large quenching; 33% in ^{20}Ne, 15% in ^{24}Mg, 27% in ^{28}Si, 47% in ^{32}S, and 52% in ^{36}Ar, respectively, compared with the USDB calculations.

Figure 12 shows the experimental and the calculated proton-neutron spin-spin correlations (8). Although the experimental data still have large error bars, the calculated results with the USDB interaction show poor agreement with the experimental data. This is also the case for the other USD interactions such as USD and USDA. The results with an enhanced IS spin-triplet pairing improve the agreement appreciably. For the IS channel, USDB* adopts the bare spin operator, while the effective spin operator $f_s^{\text{IS}} = 0.9$ is used for the USDB*qis case. The effective operator gives a smaller spin-spin correlation Δ_{spin} than the case of bare IS spin operator. The positive value of the correlation indicates that the population of spin triplet pairs in the ground state is larger than that of the spin singlet pairs. We should remind the reader that the spin and the

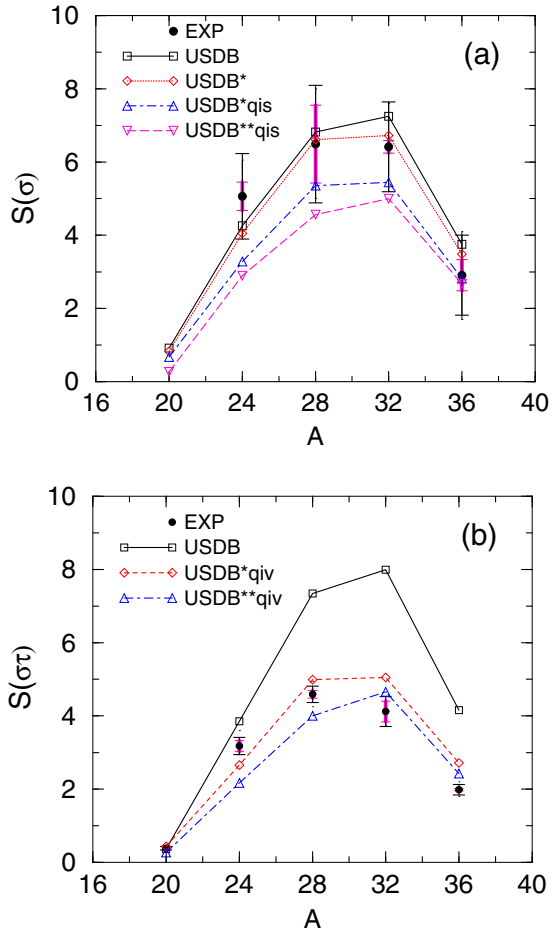

FIG. 11. Accumulated spin-$M1$ transition strengths of (a) IS channel and (b) IV channel. Experimental and theoretical data are summed up to $E_x = 16$ MeV. Shell-model calculations are performed with the USDB effective interaction: (a) In the results of USDB* and USDB*qis, the IS spin-triplet pairing interaction is enhanced by multiplying the relevant matrix elements by a factor of 1.1 compared with the original USDB interactions and the quenching factor $f_s^{\rm IS} = 1.0$ and 0.9 for IS spin operator, respectively. For USDB**qis, the IS pairing interaction is enhanced by a factor of 1.2 and a quenching factor $f_s^{\rm IS} = 0.9$ is introduced for the IS spin operator. Experimental data are taken from Ref. [29]. Long thin error bars indicate the total experimental uncertainty, while the short thick error bars denote the partial uncertainty from the spin assignment. (b) The effective IV operators are adopted for spin, orbital, and spin-tensor operators in the case of USDB*qiv and USDB**qiv. The effective operators are taken from Ref. [3]. For the results of USDB*qiv and USDB**qiv, the IS pairing interaction is enhanced by a factor of 1.1 and 1.2, respectively, with the effective operators.

spin-isospin $M1$ strengths may exist in the energy region above $E_x = 16$ MeV. In the analysis of Fig. 12, these higher-energy contributions are assumed to be the same for both the IS and IV channels. In the shell-model calculations in the full sd-shell, the spin $M1$ strength above 16 MeV is small in the $N = Z$ nuclei except ^{20}Ne and ^{24}Mg. In ^{20}Ne, 20% and 51% of the total strengths exist in the energy region $E_x =$ (16–46) MeV for the IS and IV channels, respectively. In the

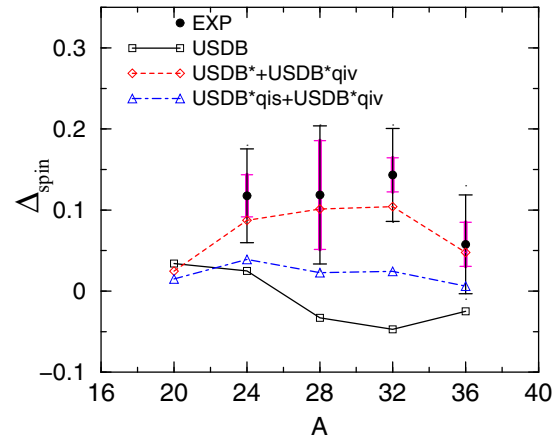

FIG. 12. Experimental and calculated proton-neutron spin-spin correlation $\Delta_{\rm spin}$ in Eq. (8). Spin $M1$ transition strengths are summed up to $E_x = 16$ MeV. Shell-model calculations are performed with an effective interaction USDB. In the results of USDB* and USDB*qis for the IS channel, the IS spin-triplet interaction is enhanced multiplying the relevant matrix elements by a factor of 1.1 compared with the original USDB, and the IS quenching factor is $f_s^{\rm IS} = 1.0$ and 0.9, respectively. The effective spin operators are used for the USDB*qiv for the IV transitions. Experimental data are taken from Ref. [29]. See the captions to Fig. 11 for the explanation of the experimental error bars.

case of ^{24}Mg, the strengths above $E_x = 16$ MeV are 9.9% and 21% of the total strengths for IS and IV channels, respectively. In the other nuclei, the spin strengths above $E_x = 16$ MeV are rather small to be a few% of the accumulated strength below $E_x = 16$ MeV and the strengths are more or less the same in both IS and IV channels. The hypothesis of equal IS and IV strengths in the higher-energy region is valid in the present theoretical calculations in nuclei $A > 28$, which should be checked experimentally in the future.

To clarify the physical mechanism of the IS spin-triplet interaction, we make a perturbative treatment of the $(2p$-$2h)$ ground-state correlations on the spin-spin matrix element. We express the wave function for the ground state with proton-neutron correlations for even-even $N = Z$ nuclei, $|\tilde{0}\rangle$, as

$$|\tilde{0}\rangle = |0\rangle + \sum_{1,1',2,2'} \alpha(1,1',2,2') \times \left|\left(1_\pi 1'^{-1}_\pi\right) J_1, T_1; \left(2_\nu 2'^{-1}_\nu\right) J_1, T_1 : J = T = 0\right\rangle. \quad (14)$$

Here the first term on the right-hand side, $|0\rangle$, is the wave function with seniority $\nu = 0$ (i.e., without the spin-triplet correlations). The second term represents the states of 2-particle-hole pairs $(1_\pi 1'^{-1}_\pi)$ and $(2_\nu 2'^{-1}_\nu)$ for proton and neutron excitations. The indices $(i \equiv 1, 2, 1', 2')$ stand for the quantum numbers of the single-particle state $i = (n_i, l_i, j_i)$. In Eq. (14), the perturbative coefficient is given by

$$\alpha(1,1',2,2') = \frac{\left\langle\left(1_\pi 1'^{-1}_\pi\right) J_1, T_1; \left(2_\nu 2'^{-1}_\nu\right) J_1, T_1 : J = T = 0\middle| H_p |0\right\rangle}{\Delta E}, \quad (15)$$

where H_p is the IS spin-triplet two-body pairing interaction and $\Delta E = E_0 - E(11'^{-1}; 22'^{-1})$. The $2p$-$2h$ states are the seniority $\nu = 4$ states in Eq. (14). The two-body matrix element in Eq. (15) is rewritten as

$$\left\langle \left(1_\pi 1_\pi'^{-1}\right) J_1, T_1; \left(2_\nu 2_\nu'^{-1}\right) J_1, T_1 : J = T = 0 \middle| H_p | 0 \right\rangle = \sum_{J_1', T_1'} \begin{Bmatrix} j_\pi & j_\pi' & J_1 \\ j_\nu' & j_\nu & J_1' \end{Bmatrix} \begin{Bmatrix} 1/2 & 1/2 & T_1 \\ 1/2 & 1/2 & T_1' \end{Bmatrix} \hat{J}_1 \hat{J}_1' \hat{T}_1 \hat{T}_1' (-)^{j_\pi' + j_\nu + J_1 + J_1' + 1 + T_1 + T_1'}$$
$$\times \left\langle (1_\pi 2_\nu) J_1', T_1'; \left(1_\pi'^{-1} 2_\nu'^{-1}\right) J_1', T_1' : J = T = 0 \middle| H_p | 0 \right\rangle,$$

where $\hat{J} \equiv \sqrt{2J+1}$ and $6j$ symbols are used (see, for example, appendixes A1 and 3B of Ref. [1] for the notations of formulas in Sec. IV). The matrix element is further expressed as

$$\left\langle (1_\pi 2_\nu) J_1', T_1'; \left(1_\pi'^{-1} 2_\nu'^{-1}\right) J_1', T_1' : J = T = 0 \middle| H_p | 0 \right\rangle = -\sqrt{2J_1 + 1} \langle (1_\pi 2_\nu) J_1', T_1' | H_p | \left(\bar{1}_\pi' \bar{2}_\nu'\right) J_1', T_1' \rangle, \tag{16}$$

where $\bar{1}_\pi'$ and $\bar{2}_\nu'$ are time-reversed states of $1_\pi'$ and $2_\nu'$, respectively. Since the pairing interaction H_p is attractive and the energy denominator ΔE is negative, the perturbative coefficient $\alpha(1, 2, 1', 2')$ should be positive. The effect of the ground-state correlations on the proton-neutron spin-spin matrix is then evaluated as

$$\langle \tilde{0} | \vec{S}_p \cdot \vec{S}_n | \tilde{0} \rangle = 2 \sum_{1,1',2,2'} \alpha(1,2,1',2') \langle 0 | \vec{S}_p \cdot \vec{S}_n \left| \left(1_\pi 1_\pi'^{-1}\right) J_1, T_1; \left(2_\nu 2_\nu'^{-1}\right) J_1, T_1 : J = T = 0 \right\rangle, \tag{17}$$

where the angular momenta and the isospins are selected to be $J_1 = 1$ and $T_1 = 0$ by the nature of the neutron-proton spin-spin matrix. The matrix element in Eq. (17) is further expressed as a reduced matrix element in the spin space,

$$\langle 0 || \vec{S}_p \cdot \vec{S}_n || \left(1_\pi 1_\pi'^{-1}\right) J_1; \left(2_\pi 2_\pi'^{-1}\right) J_1 : J = 0 \rangle = \delta_{J_1,1} \frac{1}{\sqrt{3}} (-)^{j_1 + j_2 - j_1' - j_2' - 1} \langle j_1' || \vec{s}_p || j_1 \rangle \langle j_2' || \vec{s}_n || j_2 \rangle. \tag{18}$$

In Eq. (18), the coupled angular momentum J_1 is taken as $J_1 = 1$ due to the selection rule of the spin matrix element. The isospin quantum number is discarded since it gives a trivial constant in Eq. (18).

We can obtain the effect of the IS spin-triplet pairing correlations on the proton-neutron spin-spin correlation matrix element by taking a $2p$-$2h$ configuration $j_1 = j_2 = j_< = 1d_{3/2}$ and $j_1' = j_2' = j_> = 1d_{5/2}$. Taking the spin-orbit splitting between $1d_{5/2}$ and $1d_{3/2}$ as 5 MeV and the spin-triplet pairing matrix element as -2 MeV, the α coefficient in Eq. (15) is evaluated to be 0.056. The effect on the neutron-proton spin-spin correlation becomes a large positive value, $\Delta_{\rm spin} = 0.27$. Thus, the positive value obtained by numerical results shown in Fig. 12 can be qualitatively understood by using these formulas for $2p$-$2h$ configuration mixing due to the IS spin-triplet pairing.

V. β-DECAY AND ISOSCALAR MAGNETIC MOMENTS

The effects of IS pairing and the effective spin operators are examined for the β-decay rates between mirror nuclei with $T = 1/2$ and $T_z = \pm 1/2$. The results are given in Table I for USDB, USDB**, USDBqGT, and USDB**qGT calculations. The IS spin-triplet pairing matrices are enhanced by a factor 1.2 multiplied by the relevant matrix elements and the bare spin operator is used for USDB**. The effective GT operator (11) by Towner is used for USDBqGT and USDB**qGT calculations. The r.m.s. deviations $\sigma_{\rm rms}$ between calculations and experiments are 0.37, 0.39, 0.15, and 0.16 for USDB, USDB**, USDBqGT, and USDB**qGT, respectively. We do not see any significant difference in the results between USDB and USDB** interactions.

Let us make the optimal $\chi-$ square fits with experimental data [40] by using the quenched spin factor for the GT operator. The r.m.s. deviation $\sigma_{\rm rms}$ of $q_{\rm GT}({\rm eff})^2 \times B({\rm GT; USDB})$ from $B({\rm GT; Expt.})$ becomes the minimum value 0.030 at $q_{\rm GT}({\rm eff}) = 0.78$, while that of $q_{\rm GT}({\rm eff})^2 \times {\rm B(GT; USDB^{**})}$ from $B({\rm GT; Expt.})$ becomes the minimum value 0.039 at $q_{\rm GT}({\rm eff}) = 0.77$. We obtain more or less the same quench factor for USDB and USDB**. This is because the odd nucleon in these $T = 1/2$ nuclei masks the pairing effect by the single-particle nature of the transition. The r.m.s. deviations $\sigma_{\rm rms}$ get reduced for the cases with the Towner's effective operator, USDBqGT and USDB**qGT, although they are not as small as those for the χ-squared-fit cases with the quench factor $q_{\rm GT}({\rm eff})$.

The traditional source of information for the IS spin operator comes from IS magnetic moments, i.e., the average of the magnetic moments of mirror nuclei. The IS magnetic moments are also calculated for USDB, USDB**, and USDB**qis as

TABLE I. β-decay rates between mirror nuclei with $T = 1/2$ and $T_z = \pm 1/2$. The shell-model calculations are performed by using USDB and USDB** interactions with the bare spin g factor as well as by USDBqGT and USDB**qGT with the Towner's effective GT operator (11).

A	J	USDB	USDB**	USDBqGT	USDB**qGT	Expt.
19	1/2	2.761	2.800	2.076	2.096	1.652
21	3/2	0.486	0.514	0.372	0.398	0.323
23	3/2	0.267	0.230	0.200	0.183	0.190
25	5/2	0.616	0.661	0.515	0.539	0.414
27	5/2	0.464	0.427	0.404	0.363	0.304
29	1/2	0.233	0.180	0.194	0.154	0.176
31	1/2	0.288	0.242	0.216	0.196	0.176
33	3/2	0.171	0.156	0.135	0.127	0.0577
35	3/2	0.138	0.143	0.116	0.117	0.0505
37	3/2	0.386	0.419	0.315	0.332	0.218
	$\sigma_{\rm rms}$	0.37	0.39	0.15	0.16	

TABLE II. IS magnetic moments extracted from the average of magnetic moments in mirror nuclei. The shell-model calculations are performed by using USDB, USDB**, and USDB**qis models as well as with the Towner's effective operator (9). The results with the effective operator (9), where the coefficients are obtained by chi-squared fitting procedure, are given as USDB+Towner and USDB**+Towner. The values are given in units of nuclear magneton μ_N.

A	J	USDB	USDB**	USDB**qis	USDB+Towner	USDB**+Towner	Expt.
19	1/2	0.431	0.432	0.414	0.385	0.371	0.371
21	3/2	0.869	0.870	0.858	0.850	0.853	0.862
23	3/2	0.844	0.838	0.829	0.832	0.834	
25	5/2	1.403	1.403	1.388	1.384	1.397	1.395
27	5/2	1.388	1.381	1.368	1.373	1.384	1.393
29	1/2	0.315	0.304	0.298	0.301	0.297	0.340
31	1/2	0.323	0.313	0.307	0.307	0.302	0.322
33	3/2	0.691	0.676	0.683	0.711	0.722	
35	3/2	0.676	0.679	0.686	0.715	0.724	0.727
37	3/2	0.629	0.630	0.642	0.681	0.692	
	$\sigma_{\rm rms}$	0.032	0.033	0.030	0.020	0.019	

well as for the case with Towner's effective operator (9) and tabulated in Table II. In the case of the Towner's operator which is denoted "+Towner," the IS spin-triplet pairing matrix is not enhanced. The coefficients of effective operator (9) are obtained by χ-squared fitting of the experimental IS spin expectation values of sd-shell nuclei with $T = 1/2$, 0, and 1 (Table II of Ref. [40]). The coefficients obtained are $f_s^{\rm IS} = 0.66$, $f_l^{\rm IS} = 0.05$, and $f_p^{\rm IS} = 0.06$ and the r.m.s. deviation $\sigma_{\rm rms}$ is 0.044. The results using enhanced IS spin-triplet pairing matrix elements by a factor 1.2 is also tabulated and denoted as USDB**+Towner. The $\sigma_{\rm rms}$ between the calculations and experiments shown in Table II are 0.032, 0.033, 0.030, 0.020, and 0.019 for USDB, USDB**, USDB**qis, USDB+Towner, and USDB**+Towner, respectively. The results of USDB+Towner and USDB**+Towner are close to each other with smaller r.m.s. deviations and quite satisfactory. We do not see any appreciable difference among the results of USDB, USDB* and USDB**qis, whose r.m.s. deviations are larger but only 1.5 times those of USDB+Towner and USDB* + Towner.

The IS magnetic moment is expressed by using the effective operators as [40]

$$[\mu_{\rm IS} - J/2]/\left(g_s^{\rm IS} - g_l^{\rm IS}\right) = \langle J|s_z|J\rangle + g_s^{\rm IS}/\left(g_s^{\rm IS} - g_l^{\rm IS}\right)\delta s, \tag{19}$$

where

$$\delta s = \delta_s\langle J|s_z|J\rangle + \delta_l\langle J|l_z|J\rangle + \delta_p\sqrt{8\pi}\langle J|[Y_2 \times \vec{s}\,]_0^{(1)}|J\rangle. \tag{20}$$

The effective factors δ_s, δ_l, and δ_p are essentially equivalent to the effective factors in Eq. (9) as $\delta_s = f_s^{\rm IS} - 1$, $\delta_l = f_l^{\rm IS}/2$, and $\delta_p = f_p^{\rm IS}$. Since the effects of spin and orbital contributions in Eq. (20) to the IS magnetic moment cancel largely because of different signs of δ_s and δ_l so that the net effect of the effective operators is rather small.

The summed IS and IV spin $M1$ transition strengths are tabulated in Table III for $N = Z$ sd-shell nuclei and ^{12}C. The calculated values are obtained by the USDB and USDB** interactions with the bare spin operator as well as with Towner's effective operators both for IS and IV transitions. The values of ^{12}C are for the IS state at $E_x = 12.708$ MeV and for the IV one at $E_x = 15.113$ MeV. For the summed strength, the enhanced IS interaction USDB** gives 12%–18% quenching for the IS spin transitions and 18%–24% quenching for the IV ones except ^{20}Ne (38% for IS and 40% for IV). The difference between ^{20}Ne and the other nuclei is due to the smaller accumulated values below $E_x = 16$ MeV for ^{20}Ne, i.e., the accumulated values exhaust 80% and 50% of the total strength of full model space for IS and IV channels,

TABLE III. Summed IS and IV spin $M1$ transition strengths in sd-shell nuclei and ^{12}C. Calculated and experimental values are accumulated up to $E_x = 16$ MeV. The shell-model calculations are performed by using USDB and USDB**(the IS pairing is enhanced by 20%) interactions as well as with Towner's effective operator (denoted "Towner") for USDB results. For ^{12}C, the shell-model calculations are performed with the SFO interaction with the bare spin operator. The experimental IS strength is for the state at $E_x = 12.708$ MeV, while the IV strength is for the state at $E_x = 15.113$ MeV. Experimental data are taken from Ref. [29]. The values in the bracket are experimental errors.

	S(IS)				S(IV)			
A	USDB	USDB**	USDB+Towner	Expt.	USDB	USDB**	USDB+Towner	Expt.
^{20}Ne	0.919	0.574	0.485		0.577	0.346	0.456	0.387(0.042)
^{24}Mg	4.256	3.573	2.221	5.05(1.00)	3.856	2.937	2.808	3.3(0.3)
^{28}Si	6.816	5.632	3.579	6.5(1.5)	7.340	5.593	5.256	4.6(0.35)
^{32}S	7.247	6.167	3.810	6.4(1.2)	7.993	6.554	5.734	4.2(0.45)
^{36}Ar	3.753	3.303	1.975	2.9(1.1)	4.159	3.414	2.978	2.0(0.2)
^{12}C	1.516			3.174(0.842)	1.937			1.909(0.094)

respectively, in ^{20}Ne, while more than 90% of the total strength exists below $E_x = 16$ MeV in other nuclei (except for the IV channel of ^{24}Mg; 80%). Towner's effective operators (9) and (10) give large quenched values, about 47%–48% quenching for all nuclei in the IS channel and 27%–28% quenching (21% for ^{20}Ne) for the IV channel. respectively. The experimental accumulated values of the IS strengths show minor quenching or even enhancement in ^{24}Mg compared with those of USDB results, while the IV data show a large quenching consistent with those obtained by Towner's effective operators. More quantitatively, we need a combined effect of the enhanced IS paring and the effective operators to get better agreement with the experimental values of IV channel for A $\geqq$ 28, as seen in Fig. 11. Although the IS moments are very well described by USDB+Towner and USDB**+Towner, the S(IS) values calculated with Towner's operators show large suppression compared with the experimental data. The values of accumulated strengths S(IS) are 0.485 (0.318), 2.221 (1.520), 3.579 (2.356), 3.810 (2.490), and 1.975 (1.282) for ^{20}Ne, ^{24}Mg, ^{28}Si, ^{32}S, and ^{36}Ar, respectively, for Towner's operators (USDB** + Towner).

The difference between the IS magnetic moment and the spin $M1$ transition will be clarified in the following way: The IS spin $M1$ transition is expressed as

$$\langle J|\hat{O}(\sigma)|0\rangle = \left(f_s^{\rm IS} - f_l^{\rm IS}\right)\langle J|\vec{\sigma}|0\rangle + f_p^{\rm IS}\sqrt{8\pi}\,\langle J|[Y_2 \times \vec{\sigma}]^{(1)}|0\rangle, \qquad (21)$$

where the nondiagonal matrix element of the operator $\vec{J}$ vanishes, and the effective coefficients $\delta_s = f_s^{\rm IS} - 1$ and $f_l^{\rm IS}$ have different signs so that the net effect $(f_s^{\rm IS} - f_l^{\rm IS})$ may give a large quenching effect. This is rather different from the IS magnetic moment in Eq. (19) where the effects of effective spin and orbital operators cancel largely.

VI. SUMMARY

In summary, we studied the IS and IV spin $M1$ transitions in even-even $N = Z$ sd-shell nuclei using shell-model calculations with USDB interactions in full sd-shell-model space. We introduced the effective operators for the spin and spin-isospin $M1$ operators in Eqs. (9) and (11) as well as the enhanced IS spin-triplet pairing. In general, the calculated results show good agreement with the experimental energy spectra in $N = Z$ nuclei as far as the excitation energies are concerned. Compared with the experimental $M1$ results, the accumulated IS spin strengths up to 16 MeV show small quenching effect, corresponding to the effective quenched operator $q^{\rm IS}$(eff) ~ 0.9, while a large quenching $q^{\rm IV}$(eff) ~ 0.7 is extracted for the IV channel. The similar quenching on the IS spin $M1$ transitions is obtained by the 20% enhanced IS spin-triplet pairing correlations with the bare spin operator. The enhanced IS pairing does not change much the excitation energy spectra themselves.

Positive contributions for the spin-spin correlations are found by the enhanced IS spin-triplet pairing interaction in these sd-shell nuclei. The effects of the effective spin operators and enhanced IS pairing on the β-decay rates and on the IS magnetic moments in sd-shell nuclei are also examined. The r.m.s. deviation between the calculated and experimental β-decay rates is improved by the effective operator, while the IS pairing has only a minor effect on these observables since the unpaired particle masks the effect of pairing correlations on the matrix elements.

Towner's effective spin operators work well to reproduce the accumulated experimental IV spin strength, while the quenching of the effective operators is much larger than the observed one in the IS spin channel. In the past, a large quenching of IS magnetic transition strength was suggested in the literature. However, the (p,p') data in Ref. [29] do not show any sign of the large quenching effect on the IS spin transitions. This point should be studied further experimentally by possible IS probes such as (d,d') reactions [44] together with comprehensive theoretical calculations.

ACKNOWLEDGMENTS

We would like to thank H. Matsubara for providing the experimental data. We would also like to thank M. Ichimura, A. Tamii, M. Sasano, and T. Uesaka for useful discussions. This work was supported in part by JSPS KAKENHI Grants No. JP16K05367 and No. JP15K05090.

[1] A. Bohr and B. R. Mottelson, *Nuclear Structure* (World Scientific, Singapore, 1998), Vol. I.
[2] A. Arima, K. Shimizu, W. Bentz, and H. Hyuga, *Advances in Nuclear Physics*, edited by J. W. Negele and E. Vogt (Plenum, New York, 1987), Vol. 18, p. 1.
[3] I. S. Towner, Phys. Rep. **155**, 263 (1987).
[4] C. Gaarde *et al.*, Nucl. Phys. A **369**, 258 (1981).
[5] T. Wakasa, H. Sakai, H. Okamura, H. Otsu, S. Fujita, S. Ishida, N. Sakamoto, T. Uesaka, Y. Satou, M. B. Greenfield, and K. Hatanaka, Phys. Rev. C **55**, 2909 (1997).
[6] K. Yako *et al.*, Phys. Lett. B **615**, 193 (2005).
[7] K. Yako, M. Sasano, K. Miki, H. Sakai, M. Dozono, D. Frekers, M. B. Greenfield, K. Hatanaka, E. Ihara, M. Kato, T. Kawabata, H. Kuboki, Y. Maeda, H. Matsubara, K. Muto, S. Noji, H. Okamura, T. H. Okabe, S. Sakaguchi, Y. Sakemi, Y. Sasamoto, K. Sekiguchi, Y. Shimizu, K. Suda, Y. Tameshige, A. Tamii, T. Uesaka, T. Wakasa, and H. Zheng, Phys. Rev. Lett. **103**, 012503 (2009).
[8] M. Sasano *et al.*, Phys. Rev. Lett. **107**, 202501 (2011); M. Sasano, G. Perdikakis, R. G. T. Zegers, S. M. Austin, D. Bazin, B. A. Brown, C. Caesar, A. L. Cole, J. M. Deaven, N. Ferrante, C. J. Guess, G. W. Hitt, M. Honma, R. Meharchand, F. Montes, J. Palardy, A. Prinke, L. A. Riley, H. Sakai, M. Scott, A. Stolz, T. Suzuki, L. Valdez, and K. Yako, Phys. Rev. C **86**, 034324 (2012).
[9] T. Wakasa, M. Okamoto, M. Dozono, K. Hatanaka, M. Ichimura, S. Kuroita, Y. Maeda, H. Miyasako, T. Noro, T. Saito, Y. Sakemi, T. Yabe, and K. Yako, Phys. Rev. C **85**, 064606 (2012).

[10] T. Suzuki, R. Fujimoto, and T. Otsuka, Phys. Rev. C **67**, 044302 (2003).
[11] T. Suzuki and T. Otsuka, Phys. Rev. C **78**, 061301 (2008).
[12] C. Yuan, T. Suzuki, T. Otsuka, F. Xu, and N. Tsunoda, Phys. Rev. C **85**, 064324 (2012).
[13] M. Honma, T. Otsuka, B. A. Brown, and T. Mizusaki, Phys. Rev. C **65**, 061301(R) (2002); M. Honma, *ibid.* **69**, 034335 (2004).
[14] M. Honma *et al.*, Eur. Phys. J. A **25**, 499 (2005).
[15] F. T. Avignone III, S. R. Elliott, and J. Engel, Rev. Mod. Phys. **80**, 481 (2008).
[16] S. Fantoni, A. Sarsa, and K. E. Schmidt, Phys. Rev. Lett. **87**, 181101 (2001); G. Shen, S. Gandolfi, S. Reddy, and J. Carlson, Phys. Rev. C **87**, 025802 (2013).
[17] T. Suzuki, S. Chiba, T. Yoshida, T. Kajino, and T. Otsuka, Phys. Rev. C **74**, 034307 (2006).
[18] K. Langanke, G. Martinez-Pinedo, P. vonNeumann-Cosel, and A. Richter, Phys. Rev. Lett. **93**, 202501 (2004); K. Langanke, *ibid.* **100**, 011101 (2008).
[19] H. Toki, T. Suzuki, K. Nomoto, S. Jones, and R. Hirschi, Phys. Rev. C **88**, 015806 (2013).
[20] S. Jones *et al.*, Astrophys. J. **772**, 150 (2013).
[21] T. Suzuki, H. Toki, and K. Nomoto, Astrophys. J. Lett. **817**, 163 (2016).
[22] S. Reddy, M. Prakash, J. M. Lattimer, and J. A. Pons, Phys. Rev. C **59**, 2888 (1999); A. Burrows and R. F. Sawyer, *ibid.* **58**, 554 (1998).
[23] A. Rabhi, M. A. Perez-Garcia, C. Providencia, and I. Vidana, Phys. Rev. C **91**, 045803 (2015).
[24] G. F. Bertsch and I. Hamamoto, Phys. Rev. C **26**, 1323 (1982).
[25] A. Bohr and B. R. Mottelson, Phys. Lett. B **100**, 10 (1981).
[26] M. Rho, Nucl. Phys. A **231**, 493 (1974); E. Oset and M. Rho, Phys. Rev. Lett. **42**, 47 (1979).
[27] A. Arima, in *Proceedings of the International Symposium on New Facet of Spin Giant Resonances in Nuclei*, edited by H. Sakai, H. Okamura, and T. Wakasa (University of Tokyo, 1997), p. 3.
[28] M. Ichimura, H. Sakai, and Wakasa, Prog. Part. Nucl. Phys. **56**, 446 (2006).
[29] H. Matsubara, A. Tamii, H. Nakada, T. Adachi, J. Carter, M. Dozono, H. Fujita, K. Fujita, Y. Fujita, K. Hatanaka, W. Horiuchi, M. Itoh, T. Kawabata, S. Kuroita, Y. Maeda, P. Navratil, P. vonNeumann-Cosel, R. Neveling, H. Okamura, L. Popescu, I. Poltoratska, A. Richter, B. Rubio, H. Sakaguchi, S. Sakaguchi, Y. Sakemi, Y. Sasamoto, Y. Shimbara, Y. Shimizu, F. D. Smit, K. Suda, Y. Tameshige, H. Tokieda, Y. Yamada, M. Yosoi, and J. Zenihiro, Phys. Rev. Lett. **115**, 102501 (2015); H. Matsubara and A. Tamii (private communication).
[30] W. A. Richter, S. Mkhize, and B. A. Brown, Phys. Rev. C **78**, 064302 (2008).
[31] H. Sagawa, T. Suzuki, and M. Sasano, Phys. Rev. C **94**, 041303(R) (2016).
[32] C. L. Bai, H. Sagawa, M. Sasano, T. Uesaka, K. Hagino, H. Q. Zhang, X. Z. Zhang, and F. R. Xu, Phys. Lett. B **719**, 116 (2013).
[33] Y. Fujita *et al.*, Phys. Rev. Lett. **112**, 112502 (2014).
[34] Y. Tanimura, H. Sagawa, and K. Hagino, Prog. Theor. Exp. Phys. **2014**, 053D02 (2014).
[35] H. Sagawa, C. L. Bai, and G. Colò, Phys. Scr. **91**, 083011 (2016).
[36] S. J. Q. Robinson and L. Zamick, Phys. Rev. C **66**, 034303 (2002).
[37] P. Van Isacker, J. Engel, and K. Nomura, Phys. Rev. C **96**, 064305 (2017).
[38] B. A. Brown and W. A. Richter, Phys. Rev. C **74**, 034315 (2006).
[39] B. H. Wildenthal, Prog. Part. Nucl. Phys. **11**, 5 (1984); B. A. Brown and B. H. Wildenthal, Annu. Rev. Nucl. Part. Sci. **38**, 29 (1988).
[40] B. A. Brown and B. H. Wildenthal, Phys. Rev. C **28**, 2397 (1983).
[41] C. D. Hoyle, E. G. Adelberger, J. S. Blair, K. A. Snover, H. E. Swanson, and R. D. Von Lintig, Phys. Rev. C **27**, 1244 (1983).
[42] P. von Neumann-Cosel *et al.*, Nucl. Phys. A **669**, 3 (2000).
[43] J. B. Flanz, R. S. Hicks, R. A. Lindgren, G. A. Peterson, J. Dubach, and W. C. Haxton, Phys. Rev. Lett. **43**, 1922 (1979).
[44] S. S. Zhang, J. Meng, S. G. Zhou, and G. C. Hillhouse, Phys. Rev. C **70**, 034308 (2004).